ACCEPTED BY THE ASTROPHYSICAL JOURNAL
Preprint typeset using LaTeX style emulateapj v. 10/09/06

CHANDRA LOCALIZATIONS AND SPECTRA OF *INTEGRAL* SOURCES IN THE GALACTIC PLANE

JOHN A. TOMSICK[1], SYLVAIN CHATY[2], JEROME RODRIGUEZ[2], ROLAND WALTER[3], PHILIP KAARET[4]

Accepted by the Astrophysical Journal

ABSTRACT

We report on the results of observations of hard X-ray sources in the Galactic plane with the *Chandra X-ray Observatory*. The hard X-ray "IGR" sources were discovered by the *INTEGRAL* satellite, and the goals of the *Chandra* observations are to provide sub-arcsecond localizations to obtain optical and infrared counterparts and to provide constraints on their 0.3–10 keV spectra. We obtained relatively short, $\sim$5 ks, observations for 20 IGR sources and find a bright *Chandra* source in *INTEGRAL* error circles in 12 cases. In 11 of these cases, a cross-correlation with optical and/or infrared source catalogs yields a counterpart, and the range of *J*-band magnitudes is 8.1–16.4. Also, in 4 cases, the *Chandra* X-ray spectra show evidence for absorbing material surrounding the compact object with a column density of local material in excess of 5×10^{22} cm^{-2}. We confirm that IGR J00234+6141 is a Cataclysmic Variable and IGR J14515–5542 is an Active Galactic Nucleus (AGN). We also confirm that IGR J06074+2205, IGR J10101–5645, IGR J11305–6256, and IGR J17200–3116 are High Mass X-ray Binaries (HMXBs). Our results (along with follow-up optical spectroscopy reported elsewhere) indicate that IGR J11435–6109 is an HMXB and IGR J18259–0706 is an AGN. We find that IGR J09026–4812, IGR J18214–1318, and IGR J18325–0756 may be HMXBs. In cases where we do not find a *Chandra* counterpart, the flux upper limits place interesting constraints on the luminosities of black hole and neutron star X-ray transients in quiescence.

Subject headings: stars: neutron — stars: white dwarfs — black hole physics — X-rays: stars — infrared: stars — stars: individual (IGR J00234+6141, IGR J01363+6610, IGR J06074+2205, IGR J09026–4812, IGR J10101–5645, IGR J11305–6256, IGR J11435–6109, IGR J14515–5542, IGR J17200–3116, IGR J17285–2922, IGR J17331–2406, IGR J17407–2808, IGR J17445–2747, IGR J17507–2856, IGR J18193–2542, IGR J18214–1318, IGR J18256–1035, IGR J18259–0706, IGR J18325–0756, IGR J18539+0727)

1. INTRODUCTION

The hard X-ray imaging of the Galactic plane by the *INTErnational Gamma-Ray Astrophysics Laboratory (INTEGRAL)* satellite is uncovering a large number of new or previously poorly studied "IGR" sources. In the most recent comprehensive paper on *INTEGRAL* sources, 500 sources had been detected by *INTEGRAL* in the 20–40 keV band, including 214 IGR sources (Bodaghee et al. 2007). While *INTEGRAL* provides hard X-ray images of unprecedented quality, it still only localizes sources to 1′–5′, which is not nearly adequate for reliably finding optical or IR counterparts. However, a relatively large fraction of the IGR sources are persistent, making it possible to detect the sources in the $\sim$1–10 keV band with *Chandra*, *XMM-Newton*, or *Swift*, vastly improving their localizations even with short observations with these satellites (Tomsick et al. 2006; Rodriguez et al. 2003; Rodriguez, Tomsick & Chaty 2008).

The group of IGR sources that have been identified include 49 Active Galactic Nuclei (AGN), 32 High-Mass X-ray Binaries (HMXBs), 9 Low-Mass X-ray Binaries, 9 Cataclysmic Variables (CVs), and smaller numbers of other source types (Bird et al. 2006; Bodaghee et al. 2007). Probably the biggest surprise is the large number of HMXBs as well as the properties of these systems. Many of the IGR HMXBs have large levels of intrinsic (i.e., local) absorption with $N_{\rm H} \sim 10^{23-24}$ cm^{-2} (e.g., Walter et al. 2003; Matt & Guainazzi 2003; Rodriguez et al. 2003; Combi et al. 2004; Walter et al. 2004; Beckmann et al. 2005; Walter et al. 2006), and there is evidence in several cases that a strong stellar equatorial outflow is responsible for the absorption (Filliatre & Chaty 2004; Chaty et al. 2008). In addition to the high column densities, some members of the group of IGR HMXBs exhibit other extreme properties, including the high amplitude X-ray flaring of the Supergiant Fast X-ray Transients (SFXTs, Negueruela et al. 2006; Sguera et al. 2006; Walter & Zurita Heras 2007) and neutron stars with very long, $\sim$1000–6000 s, spin periods (Patel et al. 2004; Lutovinov et al. 2005), which may, in at least some cases, be due to very high neutron star magnetic fields (Patel et al. 2007).

In order to determine the nature of more of the unclassified IGR sources, we have been obtaining observations of IGR sources in the Galactic plane with the *Chandra X-ray Observatory*. We observed 4 sources during *Chandra* observing cycle 6, obtained sub-arcsecond localizations for all 4, and found that 2 of these sources are CVs, 1 is an HMXB, and 1 is a likely HMXB (Tomsick et al. 2006; Masetti et al. 2006b; Chaty et al. 2008). When we selected targets for our cycle 8 proposal (in 2006 March), we considered all the IGR sources that had been detected at that time (now, the number has nearly doubled, and we are observing many of the recently detected sources in cycle 9). As we are interested in Galactic sources, we selected sources that are within 5° of the Galactic plane. We also eliminated sources from our list that

[1] Space Sciences Laboratory, 7 Gauss Way, University of California, Berkeley, CA 94720-7450, USA (e-mail: jtomsick@ssl.berkeley.edu)
[2] AIM - Astrophysique Interactions Multi-échelles (UMR 7158 CEA/CNRS/Université Paris 7 Denis Diderot), CEA Saclay, DSM/IRFU/Service d'Astrophysique, Bât. 709, L'Orme des Merisiers, FR-91 191 Gif-sur-Yvette Cedex, France
[3] INTEGRAL Science Data Centre, Observatoire de Genéve, Université de Genéve, Chemin d'Ecogia, 16, 1290 Versoix, Switzerland
[4] Department of Physics and Astronomy, University of Iowa, Iowa City, IA 52242, USA

were considered to be likely Active Galactic Nuclei (AGN), and this left us with a list of 20 targets.

Between 2006 December and 2008 February, we obtained cycle 8 *Chandra* observations of these 20 IGR sources. The goals of the observations are to provide a sub-arcsecond position for each source to facilitate an optical/IR identification and to obtain a soft X-ray spectrum. In the following, we describe the *Chandra* observations and our analysis of these data in §2. For the cases where we obtained sub-arcsecond *Chandra* positions, we report on the results of our search for optical and IR counterparts in §3. Then, in §4, we describe the implications for each source and give our conclusions in §5.

2. *CHANDRA* OBSERVATIONS AND ANALYSIS

2.1. Chandra *Observations*

Between 2006 December and 2008 February, we obtained cycle 8 *Chandra* observations of 20 IGR sources. The ObsIDs for these $\sim$5 ks "snapshot" observations taken with the Advanced CCD Imaging Spectrometer (ACIS, Garmire et al. 2003) are 7518–7535, 7561, and 7562, and the IGR source names and more details on the observations can be found in Table 1. For each observation, we started with a "level 1" event list produced via the *Chandra* data pipeline. We downloaded the most recent level 1 data products as of 2008 March after these were processed at the *Chandra* X-ray Center with pipeline ("ASCDS") versions between 7.6.9 and 7.6.11.1. We performed all further data processing locally using the *Chandra* Interactive Analysis of Observations (CIAO) version 4.0 software and Calibration Data Base (CALDB) version 3.4.2. For each observation, we used the CIAO routine `acis_process_events` to obtain a "level 2" event list and image. We note that while a level 2 file is produced in the pipeline data, the primary reason that we re-produced the file is so that we would be using the most recent time-dependent gain information.

Nineteen of the observations were carried out with ACIS-S, while the observation of IGR J11305–6256 (ObsID 7527) was carried out with the ACIS-I to obtain a 16-by-16 arcminute^2 continuous field-of-view (FOV) rather than the 8-by-32 arcminute^2 continuous FOV for ACIS-S with 4 CCD detectors activated. Although the FOV is more favorable for ACIS-I, ACIS-S was our first choice because of its better soft X-ray response. The radii of the *INTEGRAL* 90% confidence error circles range from $1'.1$ to $4'.8$ (Bird et al. 2007, 2006; Chenevez et al. 2004), and our *Chandra* observations covered the entire *INTEGRAL* error circle in all cases except one, IGR J00234+6141 (ObsID 7424). Although the *Chandra* FOV only covered about 80% of the IGR J00234+6141 error circle, this was a case where we detected a bright *Chandra* source in the *INTEGRAL* error circle.

2.2. *Search for Sources and X-ray Identifications*

While several of the observations show bright *Chandra* sources in their corresponding *INTEGRAL* error circles that are obvious likely counterparts, we performed a formal search for sources using CIAO program `wavdetect` (Freeman et al. 2002). In all cases (except IGR J00234+6141 as described above), the search covered the full *INTEGRAL* error circle, and the search typically extended over the ACIS chip containing the observation aimpoint (ACIS-S3). In a few cases, the *INTEGRAL* error circle extended to the adjacent chip (ACIS-S2 or ACIS-S4), and we extended the search to part or all of the adjacent chip. For the search, we used the 0.3–10 keV images and a detection threshold of 10^{-6}, which corresponds to the likely detection of 1 spurious source per ACIS chip (with 1024-by-1024 pixels per chip).

The number of *Chandra* sources detected in each *INTEGRAL* error circle varies widely from zero to 12 sources. In total, 65 sources are detected, and the sum of the error circle areas is 475 arcmin^2 for an average source density of 0.137 sources/arcmin^2. Thus, one expects 0.52 sources for the smallest $1'.1$ error circle (we detect zero) and 9.4 sources for the largest $4'.8$ error circle (we detect 12). Although one does not necessarily expect the source density to be uniform for different pointing directions through the Galaxy, our numbers of detected sources do not require large variations in the source density.

The count rates for these 65 sources also vary widely from $<1\times10^{-3}$ c/s ($<$5 counts) to nearly 0.5 c/s ($\sim$2,500 counts). The median number of counts per source is 9.6, while the mean is 141.8, indicating that there is a population of anomalously bright sources in at least some of these pointings. In fact, in 11 of our observations, there are single bright sources with count rates between 0.055 and 0.446 c/s. In our previous *Chandra* study of four IGR sources (Tomsick et al. 2006), we measured ACIS count rates between 0.039 and 0.18 c/s, so the rates for the 11 bright sources mentioned above are in-line with what we expect if these are the *Chandra* counterparts to the IGR sources. The *Chandra* positions and ACIS count rates for these sources are listed in Table 2. There is one other case where we also believe there is strong evidence that our *Chandra* observations have uncovered the correct counterpart. For IGR J18325–0756, we detect only one source in the $1'.3$ *INTEGRAL* error circle. Although this is only a 30 count source (0.0059 c/s), it is very close to the center of a relatively small *INTEGRAL* error circle, and we have listed it in Table 2 as a likely counterpart to IGR J18325–0756. The *Chandra* images for these 12 sources are shown in Figure 1.

The other 8 observations do not yield clear counterparts. In 3 cases (IGR J18539+0727, IGR J18193–2542, and IGR J17331–2406), no *Chandra* sources are detected in the *INTEGRAL* error circles. In the other 5 cases (IGR J01363+6610, IGR J17407–2808, IGR J17445–2747, IGR J17285–2922, and IGR J17331–2406), multiple (between 2 and 7) *Chandra* sources are detected, but, in each case, no one source is anomalously bright. For the *Chandra* sources detected in these observations, the numbers of ACIS counts collected are between 4 and 16. Although these faint *Chandra* sources may possibly be counterparts to the IGR sources, we do not have any basis for picking which *Chandra* source is the correct counterpart. A list of *Chandra* sources detected in the *INTEGRAL* error circles for these five observations is provided in Table 3. There are at least 3 possibilities why we are not able to find unique counterparts in these 8 cases: The IGR sources may be variable or transient; the IGR sources may be highly absorbed; or the IGR sources may lie outside of the 90% confidence *INTEGRAL* error circles we have been considering. In §4.8, we discuss each of the 8 cases where we are not able to determine a unique counterpart in more detail.

For the observations without clear counterparts, we also inspected the portion of the ACIS FOV outside of the *INTEGRAL* error circles, and there are notable sources in 2 cases. For IGR J17407–2808, the *INTEGRAL* error circle radius is $4'.2$, and we detect a very bright, $\sim$5,400 count source $6'.0$ from the center of the *INTEGRAL* error circle.

The position of this source is R.A. = $17^h40^m42^s.84$, Decl. = –28°18′08″.5 (equinox 2000.0, 90% confidence uncertainty = 0″.64), which is consistent with the location of the neutron star LMXB SLX 1737–282 (Tomsick et al. 2007c). It is clear that this *Chandra* source, CXOU J174042.8–281808 is SLX 1737–282, but it is doubtful that SLX 1737–282 and IGR J17407–2808 are the same source. The other case where there is a possible counterpart outside of the *INTEGRAL* error circle is IGR J17445–2747. While the *INTEGRAL* position is good to 2′.3, we find a 211 count source that is 4′.4 away from the best *INTEGRAL* position at R.A. = $17^h44^m46^s.02$, Decl. = –27°47′32″.7 (equinox 2000.0, 90% confidence undertainty = 0″.64). This source, CXOU 174446.0–274732, is on the edge of the 5″.1 *Swift* error circle for a source that was a suggested as a likely counterpart for IGR J17445–2747 (Landi et al. 2007). However, since both sources are well outside the *INTEGRAL* error circle, it is not clear that either of them is associated with IGR J17445–2747.

2.3. *Spectral Analysis*

We extracted 0.3–10 keV ACIS spectra for each of the 12 *Chandra* sources that have likely associations with IGR sources using the CIAO tool `psextract`. We extracted source photons from a circular region centered on each source with radii of between 5″ and 7″.5. The somewhat larger radii are necessary for the cases where the *Chandra* sources are farther off-axis causing the source photons to be spread over more pixels. We also extracted background spectra from an annulus with an inner radius of 10″ and an outer radius of 50″ centered on the source. We used the CIAO tools `mkacisrmf` and `mkarf` to produce the ACIS response matrices. While we produced spectra re-binned to 11 spectral bins in order to provide an opportunity to look for spectral features, we make use of both binned and unbinned spectra in this work.

We fitted the binned 0.3–10 keV ACIS spectra using the XSPEC v12 software with an absorbed power-law model using χ^2 statistics. To account for absorption, we used the photoelectric absorption cross sections from Balucinska-Church & McCammon (1992) and elemental abundances from Wilms, Allen & McCray (2000), which correspond to the estimated abundances for the interstellar medium. In 5 cases, we obtained very poor fits with reduced-χ^2 values of between 4 and 10 for 9 degrees of freedom (dof), and given the relatively high count rates in these cases (between 0.197 and 0.235 c/s) as well as the fact that the strongest residuals are at the high energy end of these spectra (e.g., 5–10 keV), we suspect that photon pile-up is the primary cause of the poor fits. We checked for pile-up for all 12 sources by looking at the number of counts detected above 10 keV, where the ACIS effective area is too small to expect any source photons to be collected. In the 5 cases where we suspect pile-up due to poor fits (IGR J09026–4812, IGR J11305–6256, IGR J14515–5542, IGR J17200–3116, and IGR J18214–1318), between 9 and 43 counts are detected above 10 keV compared to between 0 and 2 counts in the other 7 cases. This confirms that we must correct for pile-up for the spectra of the 5 sources listed above. Finally, we note that the count rates for IGR J00234+6141 and IGR J18259–0706 are even higher, at levels of 0.446 and 0.487 c/s, respectively. However, these two sources are also the farthest off-axis at 4–5′. With the larger off-axis point spread function the source counts are spread over more pixels, and we do not see any evidence for significant pile-up in these cases.

We re-fitted the 12 spectra using the same absorbed power-law model, but with the addition of the Davis (2001) pile-up model in the 5 cases where pile-up is significant. Also, for these fits, we used the unbinned spectra and found the best fit parameters using the Cash statistic. The results are given in Table 4, and the parameters indicate that these sources do indeed have hard spectra, which provides further confirmation that these are the counterparts to the IGR sources. For 11 sources (all except IGR J18325–0756), the best fit values for the power-law photon index are between $\Gamma = 0.1$ and 1.5, which is inconsistent with a blackbody spectrum and indicates a hard component to the spectrum. For IGR J18325–0756, only 30 counts were collected, and the spectral shape is not well-constrained as we obtain $\Gamma = 2.8^{+5.4}_{-2.7}$ (90% confidence). However, we also obtain a column density of $N_{\rm H} = (3.4^{+4.4}_{-2.3}) \times 10^{23}$ cm^{-2}, suggesting that this source may have local absorption like many of the IGR sources. In fact, several of the sources show evidence for local absorption with values of $N_{\rm H}$ that are significantly higher than the inferred column densities ($N_{\rm H}$ and $N_{\rm H_2}$) through the Galaxy along their lines of sight (see Table 4). In addition to IGR J18325–0756, sources IGR J06074+2205, IGR J11435–6109, and IGR J18214–1318 have $N_{\rm H}$ values of $(7.2^{+2.5}_{-2.0}) \times 10^{22}$, $(1.5^{+0.5}_{-0.4}) \times 10^{23}$, and $(1.17^{+0.30}_{-0.27}) \times 10^{23}$ cm^{-2}, while the Galactic $N_{\rm H}$ values for these 3 sources are between 6.1×10^{21} and 1.6×10^{22} cm^{-2} (Dickey & Lockman 1990) and the Galactic $N_{\rm H_2}$ values are between 1×10^{20} and 4×10^{21} cm^{-2}. The *Chandra* spectra are shown in Figure 2, and one can see the higher levels of absorption for these 4 sources.

To estimate possible levels of long-term variability for these 12 sources, we used the *Chandra* spectral parameters from Table 4 to compare the flux levels we are seeing with *Chandra* to the flux levels measured in the 20–40 keV band by *INTEGRAL* as reported in Bird et al. (2007). As the energy bands do not overlap, we compared the fluxes by extrapolating the *Chandra* power-law spectra into the 20–40 keV band. We note that there is one exception, IGR J06074+2205, which was only detected by *INTEGRAL* in the 3–10 keV band, so we performed the comparison in that energy band. Table 5 shows the results of the comparisons, including a calculation of the ratio of the extrapolated *Chandra* flux to the *INTEGRAL* flux. The three sources with the lowest values, IGR J06074+2205, IGR J10101–5645, and IGR J18325–0756, have ratios of 0.021 ± 0.009, 0.05 ± 0.04, and <0.03, respectively, indicating high levels of variability, and these sources might be described as transient. For the other 9 sources, the best values for the ratios are between 0.17 and 1.7, although it should be noted that most have relatively large error bars and also that determining whether a source is variable depends on our assumption about the power-law extending into the 20–40 keV band.

3. OPTICAL/IR IDENTIFICATIONS

With the *Chandra* positions for the 12 IGR sources, we searched for optical/IR counterparts in the following catalogs: the 2 Micron All-Sky Survey (2MASS); the Deep Near Infrared Survey of the Southern Sky (DENIS); and the United States Naval Observatory (USNO-B1.0), and the results of the search are given in Table 6. For each source, the table lists the 2MASS source that is closest to the *Chandra* position. Given the *Chandra* position uncertainties of 0″.64 and the 2MASS position uncertainties of 0″.2, only sources with *Chandra*/2MASS separations less than $\sim$0″.7 should be considered as possible or likely counterparts. In 11 cases, there are 2MASS sources with positions consistent with the *Chan-*

dra positions, and we consider these associations to be likely. For IGR J18256–1035, the *Chandra*/2MASS separation is 5″.7, indicating that these two sources are not associated. Figure 3 shows 2MASS *J*-band images with the *Chandra* positions marked for all 12 fields. In the case of IGR J18256–1035 (Figure 3j), it is apparent that the region is very crowded, and the *Chandra* source falls in an area where several IR sources are blended together.

The 11 sources with likely 2MASS counterparts have a wide range of brightnesses from $J = 8.0$ to $J = 16.4$. The brightest of the sources is IGR J11305–6256, and this source appears in the 2MASS, DENIS, and USNO-B1.0 catalogs at optical and IR magnitudes near 8. As discussed below, the very low extinction (J–$K_s = 0.04 \pm 0.04$) likely indicates that the source is relatively nearby. On the other hand, IGR J09026–4812, which has $J = 15.57 \pm 0.08$, shows a highly reddened spectral energy distribution with J–$K_s = 2.88 \pm 0.09$. Either extinction or a very red intrinsic spectrum (more likely the former) explain why this source is not detected in the optical (down to the USNO-B1.0 limit). Although many of the regions are too crowded to comment on whether the sources are extended in the 2MASS images or not, Figure 3g shows that IGR J14515–5542 is clearly extended. Our *Chandra* position confirms that this source is an AGN as suggested by Masetti et al. (2006b). An inspection of the other sources shown in Figure 3 does not suggest that they are extended, and many of the sources that are relatively isolated appear to be point-like.

While we believe that the association of IGR J18325–0756 with 2MASS J18322828–0756420 is likely, this is the faintest IR source in our sample ($J = 16.4$) as well as having the largest *Chandra*/2MASS separation (0″.63). Thus, in this work, we include IR observations of the IGR J18325–0756 field taken at the European Southern Observatory's 3.5 meter New Technology Telescope (ESO's NTT) at La Silla Observatory. We performed NIR photometry in J, H and K_s bands of IGR J18325–0756 on 2004 July 11 with the spectro-imager SofI (Son of Isaac). We used the large field of SofI's detector, giving an image scale of 0″.288/pixel and a field of view of 4.92 arcmin^2. We obtained the photometric observations for each filter following the standard jitter procedure. This consists of a repeating pattern of 9 different 30″ offset positions, allowing us to cleanly subtract the sky emission in NIR. The integration time was 50 s for each individual exposure, giving a total exposure time of 450 s. We observed three photometric standard stars from the faint NIR standard star catalog of Persson et al. (1998): [PMK98] 9157, [PMK98] 9172, [PMK98] 9181.

We used the Image Reduction and Analysis Facility (IRAF) suite to perform data reduction, carrying out standard procedures of NIR image reduction, including flat-fielding and NIR sky subtraction. We performed accurate astrometry using all stars from the 2MASS catalog present in the SofI field, amounting to ∼1000 2MASS objects, and the rms of astrometry fit is <0″.5. The K_s-band image is shown Figure 4, and the *Chandra* position is consistent with the position of the IR source. We carried out aperture photometry, and we then transformed instrumental magnitudes into apparent magnitudes using the standard relation: $mag_{app} = mag_{inst} - Zp - ext \times AM$, where mag_{app} and mag_{inst} are the apparent and instrumental magnitudes, Zp is the zero-point, *ext* is the extinction, and AM is the airmass. For the extinction, we used $ext_{\rm J} = 0.06$, $ext_{\rm H} = 0.04$, and $ext_{\rm Ks} = 0.10$, typical of La Silla Observatory. The apparent magnitudes are $J = 16.26 \pm 0.04$, $H = 15.13 \pm 0.06$, and $K_s = 14.27 \pm 0.08$, which are consistent with the 2MASS magnitudes.

4. DISCUSSION

Here, we discuss the implications of our results for all 20 *Chandra* observations of IGR source fields. In the 12 cases where we find likely counterparts, these represent the first time that sub-arcsecond X-ray positions have been obtained. We begin with discussions of the 6 cases where our *Chandra* positions confirm associations with previously suggested counterparts in the literature. In these cases, counterparts were previously suggested based on the presence of unusual CVs, HMXBs, or AGN in the *INTEGRAL* error circles. We then discuss the 6 cases where the *Chandra* detections either provide new optical/IR counterparts or rule out previously suggested counterparts. Finally, we discuss the 8 cases where we were not able to obtain clear *Chandra* counterparts to the IGR sources.

4.1. *Confirmations of Previously Suggested Associations*

IGR J00234+6141: The position of CXOU J002257.6+614107 is consistent with the position of the Cataclysmic Variable (CV) reported in Halpern & Mirabal (2006) and Bikmaev et al. (2006). It is also less than 6″ from the position of the *ROSAT* source 1RXS J002258.3+614111, confirming this association. It has been found that this source belongs to the Intermediate Polar CV class and contains a white dwarf with a spin period of 563.5 s and an orbital period of 4.033 h (Bonnet-Bidaud et al. 2007).

IGR J06074+2205: The position of CXOU J060726.6+220547 is consistent with the position of the Be star reported in Halpern & Tyagi (2005) and Masetti et al. (2006a), confirming that this source is a (Be-type) High-Mass X-ray Binary. In addition to the position, our study shows that there is material local to the compact object that contributes to the column density of $N_{\rm H} = (7.2^{+2.5}_{-2.0}) \times 10^{22}$ cm^{-2} that we measure in the X-ray. The fact that there must be local absorption is especially clear since the source is bright in the optical ($B = 12.7 \pm 0.3$). When the source was originally detected by *INTEGRAL* in 2003, IGR J06074+2205 was reported to have a 3–10 keV flux of 7 ± 2 mCrab (Chenevez et al. 2004), and we find that the flux during the *Chandra* observation was a factor of ∼50 lower (see Table 5). Such a flux ratio between outburst and quiescence would not be unusual for a Be X-ray binary (Campana et al. 2002), and probably indicates a binary orbit with some eccentricity.

IGR J10101–5654: The position of CXOU J101011.8–565532 is consistent with the position of the star that Masetti et al. (2006b) suggest as the possible counterpart. Masetti et al. (2006b) report an optical spectrum for this star with a strong Hα emission line and a reddened continuum, and they conclude that the star is an early-type giant. With a column density of $N_{\rm H} = (3.2^{+1.2}_{-1.0}) \times 10^{22}$ cm^{-2}, the *Chandra* spectrum does not indicate a high level of local absorption. It is notable that this is one of the sources for which the extrapolated *Chandra* flux is significantly lower than the flux measured by *INTEGRAL* (see Table 5). This indicates significant change in mass accretion rate onto the compact object, and it could point to an eccentric binary orbit.

IGR J11305–6256: The position of CXOU J113106.9–625648 is consistent with the position of the star HD 100199, which was suggested as a possible counterpart by Masetti et al. (2006c). As mentioned above, this source was the brightest companion we found with optical and IR magnitudes of ∼8. The spectral type of the star is B0IIIe, so

this system is a Be type HMXB, and Masetti et al. (2006c) estimate its distance at ∼3 kpc. The *Chandra* energy spectrum shows a low level of absorption, $N_{\rm H} = (3.2^{+2.8}_{-2.2}) \times 10^{21}$ cm^{-2}, consistent with the low optical extinction and a relatively small distance for the source. At 3 kpc, the flux reported in Table 4 corresponds to a 0.3–10 keV luminosity of $(4.7^{+2.1}_{-3.6}) \times 10^{34}$ ergs s^{-1}.

IGR J14515–5542: The position of CXOU J145133.1–554038 is consistent with the position of the Seyfert 2 Active Galactic Nucleus LEDA 3079667, which has a redshift of $z = 0.018$ (Masetti et al. 2006b). This source appears in the 2MASS catalog of extended sources as 2MASX J14513316–5540388. This source was previously observed by *Swift*, and Malizia et al. (2007) mention that this is one of five Seyfert 2 AGN in their sample with lower levels of absorption than might be expected for Seyfert 2s. We measure a slightly higher value for $N_{\rm H}$ for our *Chandra* spectrum ($(1.0^{+0.4}_{-0.3}) \times 10^{22}$ cm^{-2} for *Chandra* vs. $(0.39^{+0.18}_{-0.16}) \times 10^{22}$ cm^{-2} for *Swift*). Given that the value of $N_{\rm H}$ along this line-of-sight through the Galaxy is 5.3×10^{21} cm^{-2}, our result still confirms that the column density for this source is lower than is typically seen for Seyfert 2s.

IGR J17200–3116: The position of CXOU J172005.9–311659 is consistent with the position of the star that Masetti et al. (2006b) suggest as a possible counterpart and is also consistent with the position of the *ROSAT* source 1RXS J172006.1–311702, confirming this association. Masetti et al. (2006b) report an optical spectrum for this star with an Hα emission line and a reddened continuum, and they conclude that the system is a likely HMXB. The *Chandra* energy spectrum indicates a column density of $N_{\rm H} = (1.9^{+0.6}_{-0.5}) \times 10^{22}$ cm^{-2}. Although this is somewhat higher than the column density through the Galaxy along this line-of-sight, it does not necessarily require local absorption.

4.2. *IGR J09026–4812*

For this source, the *Chandra* observation described above in this paper led to the first X-ray position accurate enough to obtain an optical/IR identification (Tomsick et al. 2007a). We have identified CXOU J090237.3–481334 with the 2MASS and DENIS sources listed in Table 6. Although optical or IR spectra are required to confirm that it is a Galactic object, we do not see any evidence that the source is extended as might be expected for an AGN as IR-bright as this source (e.g., IGR J14515–5542). Assuming that it is a Galactic source, it is probably relatively distant or highly reddened since it has the largest J–$K_{\rm s}$ value of any of our targets as mentioned above, and it is not detected in the USNO-B1.0 catalog or in the I-band in the DENIS catalog. The J–$K_{\rm s}$ of 2.88 ± 0.09 does not fit any stellar spectral type, and must be primarily due to extinction.

If we hypothesize that the source is an HMXB, which may be required for the combination of high extinction and IR brightness, we can perform a consistency check on our hypothesis by assuming a spectral type of B0V, which has an absolute magnitude of $M_K = -2.5$. We assume that the extinction is at a level consistent with the range between the Galactic value and the X-ray value we measure (see Table 4), and this gives $A_V = 5.8$–10.6 ($A_K = 0.66$–1.21). Using $K_{\rm s} = 12.69$, we calculate a distance range of $d = 6.3$–8.1 kpc, corresponding to a 0.3–10 keV X-ray luminosity of $(8^{+13}_{-1}) \times 10^{34}$ $(d/7\ {\rm kpc})^2$ ergs s^{-1}, which is in-line with values obtained for other IGR HMXBs (and also the value of $\Gamma = 1.1^{+0.5}_{-0.3}$ for the X-ray spectral index is typical). Overall, the hypothesis of an HMXB with a main sequence companion works for IGR J09026–4812. If we instead assume a supergiant companion with $M_K = -5.9$ (B0I), we obtain a distance of 30–40 kpc, indicating that a supergiant companion is unlikely.

4.3. *IGR J11435–6109*

IGR J11435–6109 is already known to be a neutron star HMXB based on the detection of pulsations at 161.76 s, and a long-term X-ray modulation at the orbital period of 52.36 d (in't Zand & Heise 2004; Swank & Markwardt 2004; Wen et al. 2006). For this source, the *Chandra* observation described above in this paper led to the first X-ray position accurate enough to obtain an optical/IR identification (Tomsick et al. 2007b). We have identified CXOU J114400.3–610736 with the 2MASS, DENIS, and USNO sources listed in Table 6. Soon after we reported the *Chandra* position, a report of optical spectroscopy of the candidate was issued, suggesting a Be companion for this HMXB (Negueruela, Torrejón & McBride 2007). The *Chandra* spectrum indicates strong absorption with $N_{\rm H} = (1.5^{+0.5}_{-0.4}) \times 10^{23}$ cm^{-2}, possibly due to a strong stellar wind from the Be star. Finally, although Negueruela, Torrejón & McBride (2007) do not determine the stellar subclass, they calculate that if the companion is a B2Ve star, then its distance is $d > 6$ kpc. Based on the *Chandra* spectrum, this corresponds to a lower limit on the 0.3–10 keV luminosity of $>3 \times 10^{34}$ ergs s^{-1}.

4.4. *IGR J18214–1318*

For this source, the *Chandra* observation described above in this paper led to the first X-ray position accurate enough to obtain an optical/IR identification, and we have identified CXOU J182119.7–131838 with the 2MASS, DENIS, and USNO sources listed in Table 6. As shown in Figure 3i, the source is blended with several other stars, and no strong argument can be made for it being point-like or extended, so we cannot rule out the possibility that it is an AGN. If the source is Galactic, the relatively large J–K_s color value of 2.4 ± 0.1 must be caused by extinction since, as for IGR J09026–4812, such a large value does not match any spectral type. This may imply a fairly large distance, but it is notable that, unlike IGR J09026–4812, IGR J18214–1318 is detected in the optical, and IGR J18214–1318 is also somewhat brighter in the IR. Although it is unclear whether this source is an HMXB, the X-ray spectrum does show evidence for local absorption with a column density of $N_{\rm H} = (1.17^{+0.30}_{-0.27}) \times 10^{23}$ cm^{-2}, and it would not be surprising if this was due to the wind from a high-mass star. Overall, we believe that the most likely source type in this case is an HMXB, but spectral confirmation is necessary.

4.5. *IGR J18256–1035*

Previously, Landi et al. (2007) reported a *Swift* position for this source with a $4''.1$ error circle, and suggested an association between IGR J18256–1035 and the optical source USNO-B1.0 0794–399102. While our *Chandra* position agrees with the *Swift* position, we do not confirm the association with the USNO source as CXOU J182543.8–103501 is $2''.9$ away from the USNO source. The image shown in Figure 3j indicates that the region is quite crowded, and while the *Chandra* source does not fall on any of the brighter J-band sources, it does fall in a region where there is IR emission. While IGR J18256–1035 must be fainter than the nearest source in the 2MASS catalog, which has $J \sim 15$, it may

not be very much fainter than this. Considering the *Chandra* spectrum, this source is notable for having the hardest (or one of the hardest when error bars are considered) power-law indexes at $\Gamma = 0.1^{+0.5}_{-0.4}$. However, the source is not strongly absorbed, and its nature is not clear.

4.6. *IGR J18259–0706*

This source has a reported *Swift* position with an error circle of 3″.71 (Malizia et al. 2007). In fact, the position of CXOU J182557.5–071022 is 5″.1 away from the *Swift* position even though it is still very likely that they are the same source. Although the *Swift* position allows for the possibility that the bright IR source that is to the West of the *Chandra* source as shown in Figure 3k is the counterpart, the *Chandra* position indicates that the IGR source is the fainter source next to it. Follow-up optical spectroscopy was performed on this source based on the identification facilitated by our *Chandra* position. Burenin et al. (2008) report the presence of a broad and redshifted Hα emission line in the optical spectrum, indicating that the source is an AGN. Furthermore, Burenin et al. (2008) classify the source as a Seyfert 1.

4.7. *IGR J18325–0756*

Recently, Landi et al. (2008) reported a *Swift* position for this source with a 4″.1 error circle, and CXOU J183228.3–075641 has a position that is consistent. The 2MASS source that Landi et al. (2008) mention as a possible counterpart is the same source that we list in Table 6. Although the *Chandra*/2MASS position difference of 0″.625 is somewhat larger than for our other identifications, our NTT observations appear to confirm the association (see Figure 4). If the source is Galactic, the relatively large J–K_s color value of 2.0 ± 0.1 is likely due to extinction and may suggest a relatively large distance. The *Swift* spectrum that Landi et al. (2008) describe is similar to the highly absorbed spectrum we see as Landi et al. (2008) mention the possibility of a column density as high as 1.5×10^{23} cm^{-2}. Between our *Chandra* spectrum and the *Swift* spectrum, this provides evidence for local absorption in this source. An HMXB nature should be considered as a possibility in this case.

4.8. *Discussion of Sources without Clear* Chandra *Counterparts*

IGR J01363+6610: We detected 3 *Chandra* sources within the *INTEGRAL* error circle for IGR J01363+6610. All three sources are very faint, with count rates between 0.0010 and 0.0019 c/s (see Table 3), and it is not possible to tell whether any of them are the correct counterpart to the IGR source. This IGR source has been suggested to be an HMXB with a Be-type companion based on the fact that there is a Be star in the *INTEGRAL* error circle (Reig et al. 2005). While our *Chandra* field-of-view covers the location of the Be star, we do not detect any X-ray source at this position. This source is a documented transient as Grebenev et al. (2004) describe an *INTEGRAL* detection at 17 mCrab and then a non-detection with an upper limit of 11 mCrab. The source may not be extremely highly absorbed because it was detected by JEM-X during its 2004 outburst (Grebenev et al. 2004); however, the JEM-X detection was reported in the 8–15 keV band, which still allows for the possibility of significant absorption. Based on the brightest of the 3 possible *Chandra* counterparts (with a count rate of 0.0019 c/s), we have calculated an upper limit to the source flux during our *Chandra* observation. Assuming that $N_{\rm H}$ is at the Galactic value (see Table 4) and a power-law spectral shape with a photon index between Γ = 1 and 2, we calculate an upper limit on the unabsorbed 0.3–10 keV flux in the range $(3.2–4.1)\times10^{-14}$ ergs cm^{-2} s^{-1}, which corrresponds to a luminosity of $\sim 5 \times 10^{30}\ d^2_{\rm kpc}$ ergs s^{-1}, where $d_{\rm kpc}$ is the source distance in kpc. At the 2 kpc distance suggested by Reig et al. (2005) for the Be star, this would correspond to a luminosity of 2×10^{31} ergs s^{-1}, which is significantly lower than quiescent luminosities of other Be X-ray binaries (Campana et al. 2002).

IGR J17285–2922: We detected 6 *Chandra* sources within the *INTEGRAL* error circle for IGR J17285–2922 with a range of count rates between 0.0013 and 0.0030 c/s (see Table 3). It is not possible to tell whether any of them are the correct counterpart to the IGR source, and no optical counterpart has been suggested for this source. *INTEGRAL* observations of the source clearly show that the source is a transient, and when it had an outburst in 2003, its power-law spectrum with a photon index of $\Gamma \sim 2.1$ suggest the possibility that it is a black hole transient. To calculate a flux upper limit from our *Chandra* observation, we make the same assumptions as for the previous source, and find that the upper limit on the unabsorbed 0.3–10 keV flux is in the range $(5.5–6.4)\times10^{-14}$ ergs cm^{-2} s^{-1}. Such a low flux would not be surprising for a black hole transient.

IGR J17331–2406: Little is known about this source other than that it a transient that had a $\sim$9 mCrab outburst in 2004 with a hard spectrum that was fitted with a power-law with $\Gamma \sim 1.8$ (Lutovinov et al. 2004). No optical counterpart has been suggested for this source, and we did not detect any *Chandra* sources in our observation. This indicates a count rate upper limit of $\sim$0.0008 c/s, which corresponds to an upper limit on the unabsorbed 0.3–10 keV flux of $(1.0–1.5)\times10^{-14}$ ergs cm^{-2} s^{-1}. As for the previous source, such a flux level could be consistent with a black hole transient nature, but we cannot rule out other possibilities.

IGR J17407–2808: We detected 7 *Chandra* sources within the *INTEGRAL* error circle for IGR J17407–2808 with a range of count rates between 0.0011 and 0.0031 c/s. It is not possible to tell whether any of them are the correct counterpart to the IGR source, and no optical counterpart has been suggested for this source. The possible X-ray counterpart 2RXP J174040.9–280852 was suggested as a possible counterpart, but we do not detect a *Chandra* source within the 16″ error circle. The source is known to be transient, and based on *INTEGRAL* detections of short flares as bright as 800 mCrab, it was suggested that the source is a Supergiant Fast X-ray Transient (Sguera et al. 2006). The ACIS-S count rate upper limit of 0.0031 c/s from our *Chandra* observation corresponds to an upper limit on the absorbed flux of $(6.0–7.2)\times10^{-14}$ ergs cm^{-2} s^{-1}. Some other SFXTs have been shown to be quite faint in quiescence, with X-ray luminosities as low as 5×10^{32} ergs s^{-1} (in't Zand 2005), so the low *Chandra* flux for IGR J17407–2808 may be consistent with a SFXT nature. However, in this case, it should also be noted that the *INTEGRAL* error circle is relatively large for this IGR source, with a radius of 4′.2. While the *Chandra* field-of-view does fully cover the error circle, if the IGR source actually lies slightly outside of the error circle, it could have been missed.

IGR J17445–2747: We detected 2 *Chandra* sources within the *INTEGRAL* error circle for this source with count rates of 0.0008 and 0.0017 c/s, and it is not possible to tell whether either of these is the correct counterpart to the IGR source. In

fact, very little is known about this source. While it might be a transient, its flux history has not been well-documented. The suggested association with a *Swift* source is discussed above in § 2.2, and while we detect the same source with *Chandra*, the fact that both of these sources are well outside the *INTEGRAL* error circle makes the connection dubious. Assuming that the *Swift* source is not the correct counterpart, we calculate an upper limit on the 0.3–10 keV unabsorbed flux of $(4.1–4.5)\times10^{-14}$ ergs cm^{-2} s^{-1}.

IGR J17507–2856: We detected 3 *Chandra* sources within the *INTEGRAL* error circle for this source. All three sources are faint, with count rates between 0.0012 and 0.0033 c/s, and it is not possible to tell whether any of them are the correct counterpart to the IGR source. The source is called a transient by Grebenev & Sunyaev (2004), but its flux history has not been well-documented. Also, there have not been any suggestions of optical counterparts for this source. We derive an upper limit on the unabsorbed 0.3–10 keV flux of $(7.4–8.4)\times10^{-14}$ ergs cm^{-2} s^{-1}.

IGR J18193–2542: We did not detect any *Chandra* source in the *INTEGRAL* error circle for IGR J18193–2542, and its nature is unclear. The source was listed in the second IBIS catalog (Bird et al. 2006), but not the third IBIS catalog (Bird et al. 2007). It is listed as a transient in (Bodaghee et al. 2007), but its flux history is not well-known. No optical counterpart for the source has been detected. Based on a non-detection in our *Chandra* observation, we infer an upper limit on the 0.3–10 keV unabsorbed flux of between 8.9×10^{-15} and 1.4×10^{-14} ergs cm^{-2} s^{-1}.

IGR J18539+0727: There is good evidence that this source is a black hole transient as Lutovinov & Revnivtsev (2003) were able to use the *Rossi X-ray Timing Explorer (RXTE)* to measure its spectral and timing properties during its outburst. Thus, perhaps it is not too surprising that we did not detect any source in the *INTEGRAL* error circle with *Chandra* because black hole transients tend to be very faint when they are in quiescence. Based on a non-detection in our *Chandra* observation, we infer an upper limit on the 0.3–10 keV unabsorbed flux in the range $(1.7–2.0)\times10^{-14}$ ergs cm^{-2} s^{-1}, which corresponds to an X-ray luminosity limit of $<2\times10^{32}$ ergs s^{-1} if the source distance is 10 kpc.

5. CONCLUSIONS

During *Chandra* observing cycles 6 and 8, we have obtained snapshot observations of 24 IGR sources located within 5° of the Galactic plane. In 16 cases, a *Chandra* counterpart is detected, providing the first sub-arcsecond X-ray positions for these sources. Such an accurate position is required to obtain or confirm optical or IR counterparts in the crowded Galactic plane region, and a summary of the results for these 16 sources is given in Table 7. The information in the table includes the position in Galactic co-ordinates, the *J*-band magnitude, the source type, the spectral type of the optical companion for Galactic sources or the AGN type for the one AGN in our sample, and an estimate of the contribution to the column density that is local to the system. For this last quantity, $N_{\rm H,local}$, we derive a range of possible levels of local absorption from the values given in Table 4 and from Tomsick et al. (2006), where the upper limit comes from assuming that all of the measured $N_{\rm H}$ is local and the lower limit comes from subtracting the Galactic $N_{\rm H}$ and two times the Galactic $N_{\rm H_2}$ from the measured value. If the lower limit is less than or consistent with zero, then there is no evidence for local absorption, and only the upper limit is quoted. For Galactic sources, a high level of local absorption provides evidence that a strong stellar wind is enveloping the compact object.

Considering the different types of sources with *Chandra* counterparts in our sample, the HMXBs are the largest group, with 6 of the sources being spectroscopically confirmed HMXBs, and 4 of the sources being possible HMXBs. At least 3 of the confirmed HMXBs are Be X-ray binaries (IGR J06074+2205, IGR J11435–6109, and IGR J11305–6256), and the *Chandra* spectra for the first two show evidence for significant local absorption ($N_{\rm H,local}$ is in the range $(4.6–9.7)\times10^{22}$ and $(10–20)\times10^{22}$ cm^{-2} for IGR J06074+2205 and IGR J11435–6109, respectively). IGR J16207–5129 has an early-type (i.e., high-mass) supergiant companion with no evidence for local aborption, and IGR J10101–5645 and IGR J17200–3116 have early-type companions, but better optical or IR spectra are required to determine the exact spectral type.

Our determination of which of the remaining sources are possible or likely HMXBs depend on several measurements that we report in this paper. All 4 of these systems have hard X-ray spectra and none of the IR images indicate that they are extended sources. In addition, IGR J09026–4812 is bright in the IR ($K_{\rm s}\sim13$), but it shows relatively high optical/IR extinction, suggesting that it is relatively distant with a luminous companion. A similar argument based on the optical/IR magnitudes holds for IGR J18214–1318, IGR J18325–0756, and IGR J16195–4945. In addition, the evidence that IGR J18214–1318 and IGR J18325–0756 are HMXBs is stronger because of the fact that $N_{\rm H,local}$ is in the range $(7–15)\times10^{22}$ cm^{-2} for the former and in the range $(6–78)\times10^{22}$ cm^{-2} for the latter, possibly indicating a strong stellar wind.

Of the remaining 6 sources, 3 of them (IGR J00234+6141, IGR J16167–4957, and IGR J17195–4100) are spectroscopically confirmed CVs. All 3 of these sources have very low X-ray column densities and are likely to be relatively nearby. IGR J14515–5542 and IGR J18259–0706 are AGN. While IGR J14515–5542 has been spectroscopically classified as a Seyfert 2, our *Chandra* spectrum confirms an earlier *Swift* result that the X-ray column density is lower than would be expected from a Seyfert 2. The final source with a *Chandra* counterpart is IGR J18256–1035. Our results confirm that this source has a hard X-ray spectrum, but it does not necessarily have any local absorption. Also, it is in a region that is very crowded with IR sources, and better optical/IR images are necessary to determine its brightness.

Table 8 lists the remaining 8 sources without a clear *Chandra* counterpart along with the upper limits on the X-ray flux from *Chandra* as well as any information about the source type from the literature. In 3 cases (IGR J17285–2922, IGR J17331–2406, and IGR J18539+0727), there is evidence from earlier *INTEGRAL* observations that these sources are black hole candidate (BHC) X-ray transients. Such systems can be very faint in quiescence (Garcia et al. 2001; Tomsick et al. 2003), so our *Chandra* non-detections can be seen as further evidence for their BHC nature. The non-detections for the likely HMXBs, IGR J01363+6610 and IGR J17407–2808, are more surprising. While many HMXBs show high levels of variability, flux upper limits in the range of 10^{-13} to 10^{-14} ergs cm^{-2} s^{-1} are lower than expected, and may indicate that these systems are more distant or have atypical properties. Although we do not know the source type for the final 3 sources (IGR J17445–2747, IGR J17507–2856,

and IGR J18193–2542), we note that all 3 sources have locations in the vicinity of the Galactic center. This could indicate that they are part of bulge population of Low-Mass X-ray Binary (possibly BHC) transients.

JAT acknowledges partial support from *Chandra* award number GO7-8050X issued by the *Chandra X-Ray Observatory Center*, which is operated by the Smithsonian Astrophysical Observatory for and on behalf of the National Aeronautics and Space Administration (NASA), under contract NAS8-03060. JAT acknowledges partial support from a NASA *INTEGRAL* Guest Observer grant NNX07AQ13G. This work is based in part on observations collected at the European Organization for Astronomical Research in the Southern Hemisphere, Chile (ESO program 073.D-0339). This publication makes use of data products from the Two Micron All Sky Survey, which is a joint project of the University of Massachusetts and the Infrared Processing and Analysis Center/California Institute of Technology, funded by NASA and the National Science Foundation. This research makes use of the USNOFS Image and Catalogue Archive operated by the United States Naval Observatory, Flagstaff Station, the SIMBAD database, operated at CDS, Strasbourg, France, and the Deep Near Infrared Survey of the Southern Sky (DENIS).

REFERENCES

Balucinska-Church, M., & McCammon, D., 1992, ApJ, 400, 699
Beckmann, V., et al., 2005, ApJ, 631, 506
Bikmaev, I. F., & Revnivtsev, M. G., Burenin, R. A., & Sunyaev, R. A., 2006, Astronomy Letters, 32, 588
Bird, A. J., et al., 2006, ApJ, 636, 765
Bird, A. J., et al., 2007, ApJS, 170, 175
Bodaghee, A., et al., 2007, A&A, 467, 585
Bonnet-Bidaud, J. M., de Martino, D., Falanga, M., Mouchet, M., & Masetti, N., 2007, A&A, 473, 185
Burenin, R. A., Bikmaev, I. F., Revnivtsev, M. G., Tomsick, J. A., & Sazonov, S.Yu., Pavlinskiy, M. N., & Sunyaev, R. A., 2008, submitted to Astronomy Letters
Campana, S., et al., 2002, ApJ, 575, L15
Chaty, S., Rahoui, F., Foellmi, C., Tomsick, J. A., Rodriguez, J., & Walter, R., 2008, A&A, 484, astro-ph/0802.1774
Chenevez, J., Budtz-Jorgensen, C., Lund, N., Westergaard, N. J., Kretschmar, P., Rodriguez, J., Orr, A., & Hermsen, W., 2004, The Astronomer's Telegram, 223
Combi, J. A., Ribó, M., Mirabel, I. F., & Sugizaki, M., 2004, A&A, 422, 1031
Dame, T. M., Hartmann, D., & Thaddeus, P., 2001, ApJ, 547, 792
Davis, J. E., 2001, ApJ, 562, 575
Dickey, J. M., & Lockman, F. J., 1990, ARA&A, 28, 215
Filliatre, P., & Chaty, S., 2004, ApJ, 616, 469
Freeman, P. E., Kashyap, V., Rosner, R., & Lamb, D. Q., 2002, ApJS, 138, 185
Garcia, M. R., McClintock, J. E., Narayan, R., Callanan, P., Barret, D., & Murray, S. S., 2001, ApJ, 553, L47
Garmire, G. P., Bautz, M. W., Ford, P. G., Nousek, J. A., & Ricker, G. R., 2003, in X-Ray and Gamma-Ray Telescopes and Instruments for Astronomy. Edited by Joachim E. Truemper, Harvey D. Tananbaum. Proceedings of the SPIE, 4851, 28
Grebenev, S. A., & Sunyaev, R. A., 2004, The Astronomer's Telegram, 342
Grebenev, S. A., Ubertini, P., Chenevez, J., Orr, A., & Sunyaev, R. A., 2004, The Astronomer's Telegram, 275
Halpern, J. P., & Mirabal, N., 2006, The Astronomer's Telegram, 709
Halpern, J. P., & Tyagi, S., 2005, The Astronomer's Telegram, 682
in't Zand, J., & Heise, J., 2004, The Astronomer's Telegram, 362
in't Zand, J. J. M., 2005, A&A, 441, L1
Landi, R., et al., 2007, The Astronomer's Telegram, 1273
Landi, R., Masetti, N., Sguera, V., Bazzano, A., Fiocchi, M., Bird, A. J., & Dean, A. J., 2008, The Astronomer's Telegram, 1423
Lutovinov, A., Bel, M. C., Belanger, G., Goldwurm, A., Budtz-Jorgensen, C., Mowlavi, N., Paul, J., & Orr, A., 2004, The Astronomer's Telegram, 328
Lutovinov, A., Rodriguez, J., Revnivtsev, M., & Shtykovskiy, P., 2005, A&A, 433, L41
Lutovinov, A. A., & Revnivtsev, M. G., 2003, Astronomy Letters, 29, 719
Malizia, A., et al., 2007, ApJ, 668, 81
Masetti, N., et al., 2006a, A&A, 455, 11
Masetti, N., et al., 2006b, A&A, 459, 21
Masetti, N., et al., 2006c, A&A, 449, 1139
Matt, G., & Guainazzi, M., 2003, MNRAS, 341, L13
Negueruela, I., Smith, D. M., Reig, P., Chaty, S., & Torrejón, J. M., 2006, in ESA SP-604: The X-ray Universe 2005, ed. A. Wilson, 165
Negueruela, I., Torrejón, J. M., & McBride, V., 2007, The Astronomer's Telegram, 1239
Patel, S. K., et al., 2004, ApJ, 602, L45
Patel, S. K., et al., 2007, ApJ, 657, 994
Persson, S. E., Murphy, D. C., Krzeminski, W., Roth, M., & Rieke, M. J., 1998, AJ, 116, 2475
Reig, P., Negueruela, I., Papamastorakis, G., Manousakis, A., & Kougentakis, T., 2005, A&A, 440, 637
Rodriguez, J., Tomsick, J. A., & Chaty, S., 2008, A&A, 482, 731
Rodriguez, J., Tomsick, J. A., Foschini, L., Walter, R., Goldwurm, A., Corbel, S., & Kaaret, P., 2003, A&A, 407, L41
Sguera, V., et al., 2006, ApJ, 646, 452
Swank, J. H., & Markwardt, C. B., 2004, The Astronomer's Telegram, 359
Tomsick, J. A., Chaty, S., Rodriguez, J., Foschini, L., Walter, R., & Kaaret, P., 2006, ApJ, 647, 1309
Tomsick, J. A., Chaty, S., Rodriguez, J., & Walter, R., 2007a, The Astronomer's Telegram, 1018
Tomsick, J. A., Chaty, S., Rodriguez, J., Walter, R., & Kaaret, P., 2007b, The Astronomer's Telegram, 1231
Tomsick, J. A., et al., 2003, ApJ, 597, L133
Tomsick, J. A., Walter, R., Kaaret, P., Rodriguez, J., & Chaty, S., 2007c, The Astronomer's Telegram, 1189
Walter, R., et al., 2004, in 5th INTEGRAL Workshop on the INTEGRAL Universe, ed. V. Schoenfelder, G. Lichti, C. Winkler, Vol. 552, 417
Walter, R., et al., 2003, A&A, 411, L427
Walter, R., & Zurita Heras, J., 2007, A&A, 476, 335
Walter, R., et al., 2006, A&A, 453, 133
Weisskopf, M. C., 2005, astro-ph/0503091
Wen, L., Levine, A. M., Corbet, R. H. D., & Bradt, H. V., 2006, ApJS, 163, 372
Wilms, J., Allen, A., & McCray, R., 2000, ApJ, 542, 914

TABLE 1
Chandra OBSERVATIONS

IGR Name	ObsID	l^a	b^b	Start Time	Exposure Time (s)
J00234+6141	7524	119.62	–1.00	2007 Mar 26, 3.18 h UT	4891
J01363+6610	7533	127.45	+3.70	2007 Jun 8, 4.16 h UT	4976
J06074+2205	7520	188.39	+0.80	2006 Dec 2, 12.52 h UT	4935
J09026–4812	7525	268.88	–1.09	2007 Feb 5, 0.36 h UT	4692
J10101–5645	7519	282.24	–0.67	2007 Jun 9, 9.98 h UT	4698
J11305–6256	7527	293.87	–1.49	2007 Sept 27, 2.22 h UT	5058
J11435–6109	7523	296.05	+0.97	2007 Sept 23, 10.14 h UT	5093
J14515–5542	7531	319.34	+3.29	2007 May 16, 7.23 h UT	4888
J17200–3116	7532	355.02	+3.35	2007 Sept 30, 22.40 h UT	4692
J17285–2922	7530	357.64	+2.88	2008 Feb 8, 19.45 h UT	4698
J17331–2406	7535	2.61	+4.93	2008 Feb 5, 6.72 h UT	5106
J17407–2808	7526	0.10	+1.34	2007 Aug 1, 13.08 h UT	5109
J17445–2747	7521	0.86	+0.81	2008 Feb 8, 17.57 h UT	4888
J17507–2856	7562	0.58	–0.96	2008 Feb 5, 8.52 h UT	4695
J18193–2542	7534	6.51	–4.91	2008 Feb 16, 3.89 h UT	5084
J18214–1318	7561	17.73	+0.47	2008 Feb 14, 13.06 h UT	4692
J18256–1035	7522	20.58	+0.84	2008 Feb 14, 11.48 h UT	4698
J18259–0706	7528	23.64	+2.35	2008 Feb 14, 9.70 h UT	4698
J18325–0756	7518	23.72	+0.56	2008 Feb 26, 22.79 h UT	5061
J18539+0727	7529	39.85	+2.85	2007 Feb 19, 11.23 h UT	4656

[a]Galactic longitude in degrees.
[b]Galactic latitude in degrees.

TABLE 2
Chandra IDENTIFICATIONS

IGR Name[a]	*Chandra* R.A. (J2000)	*Chandra* Decl. (J2000)	*Chandra*/ACIS Count Rate
J00234+6141	$00^h22^m57^s.64$	$+61°41'07''.5$	0.446
J06074+2205	$06^h07^m26^s.62$	$+22°05'47''.6$	0.064
J09026–4812	$09^h02^m37^s.33$	$-48°13'34''.1$	0.235
J10101–5645	$10^h10^m11^s.87$	$-56°55'32''.1$	0.055
J11305–6256	$11^h31^m06^s.95$	$-62°56'48''.9$	0.203
J11435–6109	$11^h44^m00^s.31$	$-61°07'36''.5$	0.074
J14515–5542	$14^h51^m33^s.15$	$-55°40'38''.4$	0.223
J17200–3116	$17^h20^m05^s.92$	$-31°16'59''.4$	0.215
J18214–1318	$18^h21^m19^s.76$	$-13°18'38''.9$	0.197
J18256–1035	$18^h25^m43^s.83$	$-10°35'01''.9$	0.057
J18259–0706	$18^h25^m57^s.58$	$-07°10'22''.8$	0.487
J18325–0756	$18^h32^m28^s.32$	$-07°56'41''.7$	0.0059

[a]For all sources, the largest contribution to the uncertainties in the *Chandra* positions are due to pointing systematics. The pointing uncertainties are $0''.64$ at 90% confidence and $1''$ at 99% confidence (Weisskopf 2005). The statistical position uncertainties are between $0''.02$ and $0''.11$.

TABLE 3
Chandra SOURCE LIST FOR CASES WITHOUT A CLEAR COUNTERPART

CXOU Name[a]	*Chandra* R.A. (J2000)	*Chandra* Decl. (J2000)	*Chandra*/ACIS Count Rate
IGR J01363+6610			
J013609.9+661157	$01^h36^m09^s.99 \pm 0^s.03$	$+66°11'57''.5 \pm 0''.2$	0.0010
J013621.2+660928	$01^h36^m21^s.22 \pm 0^s.06$	$+66°09'28''.7 \pm 0''.2$	0.0012
J013632.8+660924	$01^h36^m32^s.84 \pm 0^s.07$	$+66°09'24''.3 \pm 0''.2$	0.0019
IGR J17285–2922			
J172830.1–292334	$17^h28^m30^s.18 \pm 0^s.02$	$-29°23'34''.7 \pm 0''.2$	0.0019
J172830.5–291946	$17^h28^m30^s.59 \pm 0^s.01$	$-29°19'46''.6 \pm 0''.2$	0.0013
J172831.1–292250	$17^h28^m31^s.17 \pm 0^s.02$	$-29°22'50''.9 \pm 0''.2$	0.0023
J172834.2–292458	$17^h28^m34^s.22 \pm 0^s.01$	$-29°24'58''.0 \pm 0''.2$	0.0016
J172836.5–291926	$17^h28^m36^s.52 \pm 0^s.02$	$-29°19'26''.2 \pm 0''.2$	0.0018
J172837.8–292133	$17^h28^m37^s.80 \pm 0^s.01$	$-29°21'33''.6 \pm 0''.1$	0.0030
IGR J17407–2808			
J174024.9–281243	$17^h40^m24^s.95 \pm 0^s.03$	$-28°12'43''.5 \pm 0''.3$	0.0023
J174031.5–281326	$17^h40^m31^s.58 \pm 0^s.02$	$-28°13'26''.8 \pm 0''.3$	0.0013
J174032.3–281042	$17^h40^m32^s.34 \pm 0^s.04$	$-28°10'42''.0 \pm 0''.2$	0.0031
J174036.4–280840	$17^h40^m36^s.41 \pm 0^s.04$	$-28°08'40''.3 \pm 0''.3$	0.0026
J174043.2–281601	$17^h40^m43^s.27 \pm 0^s.02$	$-28°16'01''.3 \pm 0''.3$	0.0026
J174044.7–281159	$17^h40^m44^s.74 \pm 0^s.02$	$-28°11'59''.5 \pm 0''.2$	0.0012
J174054.6–280949	$17^h40^m54^s.60 \pm 0^s.01$	$-28°09'49''.5 \pm 0''.5$	0.0011
IGR J17445–2747			
J174427.3–274324	$17^h44^m27^s.33 \pm 0^s.03$	$-27°43'24''.1 \pm 0''.4$	0.0008
J174435.4–274453	$17^h44^m35^s.40 \pm 0^s.01$	$-27°44'53''.3 \pm 0''.2$	0.0017
IGR J17507–2856			
J175036.7–285452	$17^h50^m36^s.76 \pm 0^s.02$	$-28°54'52''.6 \pm 0''.3$	0.0030
J175045.3–285817	$17^h50^m45^s.30 \pm 0^s.02$	$-28°58'17''.0 \pm 0''.4$	0.0012
J175049.7–285510	$17^h50^m49^s.74 \pm 0^s.02$	$-28°55'10''.7 \pm 0''.2$	0.0033

[a]For all sources, the position errors given in the table are the 1-σ statistical errors calculated by the `wavdetect` software. A systematic pointing uncertainty should be added to this. The pointing uncertainties are $0''.64$ at 90% confidence and $1''$ at 99% confidence (Weisskopf 2005).

TABLE 4
Chandra SPECTRAL RESULTS

IGR Name[a]	N_H ($\times 10^{22}$ cm^{-2})	Γ	X-ray Flux[b]	α^c	PSF Fraction[d]	Fit Statistic[e]	Galactic N_H/N_{H_2} ($\times 10^{22}$ cm^{-2})[f]
J00234+6141	$0.17^{+0.05}_{-0.04}$	0.87 ± 0.09	8.6 ± 0.5	–	–	631.8/660	0.73/0.0009
J06074+2205	$7.2^{+2.5}_{-2.0}$	0.9 ± 0.5	$3.5^{+0.8}_{-0.5}$	–	–	548.1/660	0.61/0.01
J09026–4812	$1.9^{+0.6}_{-0.4}$	$1.1^{+0.5}_{-0.3}$	13^{+23}_{-2}	$0.66^{+0.30}_{-0.24}$	$0.85^{+0.03}_{-0.00}$	778.3/658	1.0/0.8
J10101–5645	$3.2^{+1.2}_{-1.0}$	$1.0^{+0.5}_{-0.4}$	$2.03^{+0.35}_{-0.25}$	–	–	465.9/660	1.8/0.8
J11305–6256	$0.32^{+0.28}_{-0.22}$	$0.33^{+0.40}_{-0.28}$	44^{+20}_{-34}	$0.78^{+0.22}_{-0.20}$	$0.91^{+0.09}_{-0.06}$	783.6/658	1.5/0.06
J11435–6109	15^{+5}_{-4}	1.1 ± 0.6	$9.1^{+4.8}_{-1.7}$	–	–	474.4/660	1.0/0.02
J14515–5542	$1.0^{+0.4}_{-0.3}$	$1.5^{+0.9}_{-0.6}$	14^{+15}_{-7}	$0.66^{+0.34}_{-0.14}$	$0.91^{+0.07}_{-0.05}$	790.8/658	0.53/0.002
J17200–3116	$1.9^{+0.6}_{-0.5}$	$0.8^{+0.5}_{-0.4}$	26^{+39}_{-16}	$0.45^{+0.55}_{-0.10}$	$0.87^{+0.03}_{-0.02}$	727.7/658	0.49/0.07
J18214–1318	$11.7^{+3.0}_{-2.7}$	$0.7^{+0.6}_{-0.5}$	60^{+317}_{-35}	$0.36^{+0.64}_{-0.10}$	$0.87^{+0.04}_{-0.02}$	634.2/658	1.6/0.4
J18256–1035	$3.1^{+1.6}_{-1.2}$	$0.1^{+0.5}_{-0.4}$	$2.9^{+0.5}_{-0.4}$	–	–	503.5/660	1.4/0.2
J18259–0706	1.7 ± 0.2	1.02 ± 0.13	14.3 ± 0.6	–	–	682.9/660	0.71/0.4
J18325–0756	34^{+44}_{-23}	$2.8^{+5.4}_{-2.7}$	$6.0^{+1.8\times10^7}_{-5.5}$	–	–	155.4/660	1.8/1.7

[a]The parameters are for power-law fits to the *Chandra*/ACIS spectra and include photoelectric absorption with Wilms, Allen & McCray (2000) abundances. A pile-up correction was applied in the cases where pile-up parameters are given. We performed fits without re-binning the data and using Cash statistics. Errors in this table are at the 90% confidence level ($\Delta C = 2.7$).

[b]Unabsorbed 0.3–10 keV flux in units of 10^{-12} erg cm^{-2} s^{-1}.

[c]The grade migration parameter in the pile-up model (Davis 2001). The probability that n events will be piled together but will still be retained after data filtering is α^{n-1}.

[d]The fraction of the point spread function (PSF) treated for pile-up (see Davis 2001). This parameter is required to be in the range 0.85–1.0.

[e]The Cash statistic and degrees of freedom for the best fit model.

[f]The atomic hydrogen column density through the Galaxy from Dickey & Lockman (1990). We also give the molecular hydrogen column density through the Galaxy, using a CO map and conversion to N_{H_2} (Dame, Hartmann & Thaddeus 2001).

TABLE 5
COMPARISON BETWEEN *INTEGRAL* AND *Chandra* FLUXES

IGR Name	Marked as Transient in the IBIS Catalog	Flux measured by *INTEGRAL*[a]	Flux Extrapolated from *Chandra* Spectra[b]	Flux Ratio[c]
J00234+6141	N	$(3.8 \pm 0.8) \times 10^{-11}$	$(2.3 \pm 0.4) \times 10^{-11}$	0.61 ± 0.17
J06074+2205[d]	Y	$(1.3 \pm 0.4) \times 10^{-10}$	$(2.6 \pm 0.7) \times 10^{-12}$	0.021 ± 0.009
J09026–4812	N	$(9.8 \pm 0.8) \times 10^{-11}$	$(2.2^{+4.3}_{-1.8}) \times 10^{-11}$	$0.22^{+0.44}_{-0.18}$
J10101–5645	N	$(8.3 \pm 0.8) \times 10^{-11}$	$(4.2 \pm 3.4) \times 10^{-12}$	0.05 ± 0.04
J11305–6256	N	$(3.0 \pm 0.1) \times 10^{-10}$	$(3.1 \pm 2.4) \times 10^{-10}$	1.0 ± 0.8
J11435–6109	N	$(9.1 \pm 1.5) \times 10^{-11}$	$(1.5^{+2.0}_{-1.5}) \times 10^{-11}$	$0.17^{+0.23}_{-0.17}$
J14515–5542	N	$(6.8 \pm 0.8) \times 10^{-11}$	$(9.9^{+20.3}_{-9.9}) \times 10^{-12}$	$0.15^{+0.30}_{-0.15}$
J17200–3116	Y	$(2.1 \pm 0.1) \times 10^{-10}$	$(7.9^{+13.5}_{-7.9}) \times 10^{-11}$	$0.38^{+0.64}_{-0.38}$
J18214–1318	Y	$(1.3 \pm 0.1) \times 10^{-10}$	$(2.2^{+11.8}_{-2.2}) \times 10^{-10}$	$1.7^{+5.4}_{-1.7}$
J18256–1035	N	$(7.6 \pm 0.8) \times 10^{-11}$	$(3.0 \pm 2.2) \times 10^{-11}$	0.39 ± 0.29
J18259–0706	N	$(7.6 \pm 0.8) \times 10^{-11}$	$(2.8 \pm 0.7) \times 10^{-11}$	0.37 ± 0.10
J18325–0756	Y	$(1.9 \pm 0.1) \times 10^{-10}$	$<5 \times 10^{-12}$[e]	<0.03

[a] The 20–40 keV (or 3–10 keV in the case of IGR J06074+2205) *INTEGRAL* fluxes in ergs cm^{-2} s^{-1} from the IBIS Catalog (Bird et al. 2007).

[b] These fluxes, in ergs cm^{-2} s^{-1}, are calculated by extrapolating the power-law fits to the *Chandra* spectra from Table 4 into the 20–40 keV band (or into the 3–10 keV band for IGR J06074+2205).

[c] The ratio of the extrapolated flux from the *Chandra* spectra to the flux measured by *INTEGRAL*.

[d] This source was detected as a transient by JEM-X (Chenevez et al. 2004) in the 3–10 keV band. It has not been detected by IBIS, and does not appear in the IBIS catalog.

[e] In this case, the large errors on the *Chandra* power-law parameters make a robust extrapolation into the 20–40 keV band impossible. This upper limit corresponds to the case of $\Gamma = 0.1$, which is the hardest power-law index consistent with the *Chandra* spectrum.

TABLE 6
OPTICAL/INFRARED IDENTIFICATIONS

Catalog/Source[a]	Separation	Magnitudes		
IGR J00234+6141/CXOU J002257.6+614107				
2MASS J00225764+6141075	0″.090	$J = 15.122 \pm 0.048$	$H = 15.046 \pm 0.082$	$K_s = 14.770 \pm 0.124$
USNO-B1.0 1516–0012283	0″.325	$B = 18.0 \pm 0.3$	$R = 16.3 \pm 0.3$	$I = 15.6 \pm 0.3$
IGR J06074+2205/CXOU J060726.6+220547				
2MASS J06072661+2205477	0″.227	$J = 10.491 \pm 0.021$	$H = 10.189 \pm 0.022$	$K_s = 9.961 \pm 0.019$
USNO-B1.0 1120–0112757	0″.467	$B = 12.7 \pm 0.3$	$R = 11.3 \pm 0.3$	$I = 10.2 \pm 0.3$
IGR J09026–4812/CXOU J090237.3–481334				
2MASS J09023731–4813339	0″.181	$J = 15.568 \pm 0.081$	$H = 13.863 \pm 0.071$	$K_s = 12.687 \pm 0.040$
DENIS J090237.3–481334	0″.451	—	$J = 15.831 \pm 0.17$	$K_s = 13.011 \pm 0.15$
IGR J10101–5654/CXOU J101011.8–565532				
2MASS J10101186–5655320	0″.006	$J = 12.617 \pm 0.044$	$H = 11.480 \pm 0.041$	$K_s = 10.669 \pm 0.029$
DENIS J101011.8–565532	0″.413	$I = 15.632 \pm 0.06$	$J = 12.506 \pm 0.07$	$K_s = 10.657 \pm 0.07$
IGR J11305–6256/CXOU J113106.9–625648				
2MASS J11310691–6256489	0″.243	$J = 8.048 \pm 0.023$	$H = 8.067 \pm 0.031$	$K_s = 8.009 \pm 0.029$
DENIS J113106.9–625649	0″.279	$I = 8.977 \pm 0.04$	$J = 8.154 \pm 0.05$	$K_s = 8.111 \pm 0.05$
USNO-B1.0 0270–0309619	0″.246	$B = 8.2 \pm 0.3$	$R = 8.2 \pm 0.3$	$I = 8.2 \pm 0.3$
IGR J11435–6109/CXOU J114400.3–610736				
2MASS J11440030–6107364	0″.082	$J = 13.003 \pm 0.022$	$H = 12.338 \pm 0.021$	$K_s = 11.852 \pm 0.019$
DENIS J114400.2–610736	0″.397	$I = 14.507 \pm 0.03$	$J = 13.019 \pm 0.08$	$K_s = 11.808 \pm 0.10$
USNO-B1.0 0288–0337502	0″.494	$B = 16.6 \pm 0.3$	$R = 15.7 \pm 0.3$	$I = 14.8 \pm 0.3$
IGR J14515–5542/CXOU J145133.1–554038				
2MASX J14513316–5540388	0″.140	$J = 11.142 \pm 0.066$	$H = 10.045 \pm 0.045$	$K_s = 9.736 \pm 0.050$
USNO-B1.0 0343–0472749	0″.195	$B = 16.3 \pm 0.3$	$R = 12.7 \pm 0.3$	$I = 12.8 \pm 0.3$
IGR J17200–3116/CXOU J172005.9–311659				
2MASS J17200591–3116596	0″.269	$J = 13.581 \pm 0.056$	$H = 12.334 \pm 0.057$	$K_s = 11.983 \pm 0.043$
DENIS J172005.9–311659	0″.353	$I = 16.212 \pm 0.07$	$J = 13.553 \pm 0.09$	$K_s = 11.938 \pm 0.08$
IGR J18214–1318/CXOU J182119.7–131838				
2MASS J18211975–1318388	0″.075	$J = 12.786 \pm 0.052$	$H = 11.657 \pm 0.099$	$K_s = 10.359$
DENIS J182119.7–131838	0″.255	$I = 17.007 \pm 0.11$	$J = 12.757 \pm 0.12$	$K_s = 10.639 \pm 0.14$
USNO-B1.0 0766–0475700	0″.574	—	$R = 20.3 \pm 0.3$	$I = 17.0 \pm 0.3$
IGR J18256–1035/CXOU J182543.8–103501				
2MASS J18254409–1035059	5″.698	$J = 15.015 \pm 0.091$	$H = 13.935 \pm 0.077$	$K_s = 13.520 \pm 0.078$
IGR J18259–0706/CXOU J182557.5–071022				
2MASS J18255759–0710229	0″.279	$J = 15.213 \pm 0.151$	$H = 13.900 \pm 0.151$	$K_s = 12.994 \pm 0.093$
IGR J18325–0756/CXOU J183228.3–075641				
2MASS J18322828–0756420	0″.625	$J = 16.398 \pm 0.177$	$H = 15.267 \pm 0.131$	$K_s = 14.490$

[a]The catalogs are the 2 Micron All-Sky Survey (2MASS), the Deep Near Infrared Survey of the Southern Sky (DENIS), and the United States Naval Observatory (USNO-B1.0). For IGR J18256–1035 we did not find a good 2MASS/*Chandra* association, and we listed the closest 2MASS source.

TABLE 7
SUMMARY OF RESULTS FOR SOURCES WITH *Chandra* COUNTERPARTS

IGR Name	l^a	b^b	*J*-band Magnitude	Source Type[d]	Spectral Type	$N_{\rm H,local}{}^c$ (10^{22} cm^{-2})
Chandra cycle 8						
J00234+6141	119.62	–1.00	15.12 ± 0.05	CV	Low Mass	<0.22
J06074+2205	188.39	+0.80	10.49 ± 0.02	HMXB	Be	5–10
J09026–4812	268.88	–1.09	15.57 ± 0.08	HMXB?	?	<2.5
J10101–5645	282.24	–0.67	12.62 ± 0.04	HMXB	Early Giant	<4.4
J11305–6256	293.87	–1.49	8.05 ± 0.02	HMXB	B0IIIe	<0.60
J11435–6109	296.05	+0.97	13.00 ± 0.02	HMXB	Be	10–20
J14515–5542	319.34	+3.29	11.14 ± 0.07	AGN	Seyfert 2	0.2–1.4
J17200–3116	355.02	+3.35	13.58 ± 0.06	HMXB	High Mass	0.8–2.5
J18214–1318	17.73	+0.47	12.79 ± 0.05	HMXB?	?	7–15
J18256–1035	20.58	+0.84	>15.0	?	?	0.1–4.7
J18259–0706	23.64	+2.35	15.21 ± 0.15	AGN	Seyfert 1	<1.9
J18325–0756	23.72	+0.56	16.26 ± 0.04	HMXB?	?	6–78
Chandra cycle 6						
J16167–4957[e]	333.06	+0.50	14.86 ± 0.06	CV	Low Mass	<0.8
J16195–4945[d]	333.56	+0.34	13.57 ± 0.03	HMXB?	?	1.1–12
J16207–5129[d]	332.46	–1.05	10.44 ± 0.02	HMXB	Early Supergiant	<5.1
J17195–4100[d]	326.98	–2.14	14.1 ± 0.1	CV	Low Mass	<0.21

[a]Galactic longitude in degrees.
[b]Galactic latitude in degrees.
[c]The estimate for the column density due to material local to the source based on a calculation of the measured $N_{\rm H}$ minus the Galactic $N_{\rm H}$ minus two times the Galactic $N_{\rm H_2}$. An upper limit indicates no evidence for local absorption, and a range indicates evidence for slight or significant local absorption.
[d]CV = Cataclysmic Variable, HMXB = High-Mass X-ray Binary, AGN = Active Galactic Nucleus.
[e]We obtained *Chandra* observations for these 4 sources in cycle 6, and we reported the results in Tomsick et al. (2006). We include these here to allow for comparison to the cycle 8 results, which are the focus of this paper. For 3 of these sources, the source type has been confirmed spectroscopically (Masetti et al. 2006b).

TABLE 8
SUMMARY OF RESULTS FOR 8 SOURCES WITHOUT CLEAR *Chandra* COUNTERPARTS

IGR Name	l^a	b^b	*Chandra* Flux Upper Limit[c]	Number of Sources Detected[d]	Source Type[e]
J01363+6610	127.45	+3.70	$<(3.2\text{–}4.1)\times10^{-14}$	3	HMXB? Be?
J17285–2922	357.64	+2.88	$<(5.5\text{–}6.4)\times10^{-14}$	6	BHC?
J17331–2406	2.61	+4.93	$<(1.0\text{–}1.5)\times10^{-14}$	0	BHC?
J17407–2808	0.10	+1.34	$<(6.0\text{–}7.2)\times10^{-14}$	7	SFXT?
J17445–2747	0.86	+0.81	$<(4.1\text{–}4.5)\times10^{-14}$	2	?
J17507–2856	0.58	–0.96	$<(7.4\text{–}8.4)\times10^{-14}$	3	?
J18193–2542	6.51	–4.91	$<(0.9\text{–}1.4)\times10^{-14}$	0	?
J18539+0727	39.85	+2.85	$<(1.7\text{–}2.0)\times10^{-14}$	0	BHC

[a]Galactic longitude in degrees.
[b]Galactic latitude in degrees.
[c]Upper limit on the 0.3–10 keV unabsorbed X-ray flux in units of ergs cm^{-2} s^{-1}. In each case, the spectral shape assumed to calculate the upper limit is an absorbed power-law with the column density at the Galactic value. The range of upper limits correspond to a range of assumed power-law photon indeces between Γ = 1 and 2.
[d]The number of *Chandra* sources detected in the 90% confidence *INTEGRAL* error circle.
[e]HMXB = High-Mass X-ray Binary, BHC = Black Hole Candidate, SFXT = Supergiant Fast X-ray Transient.

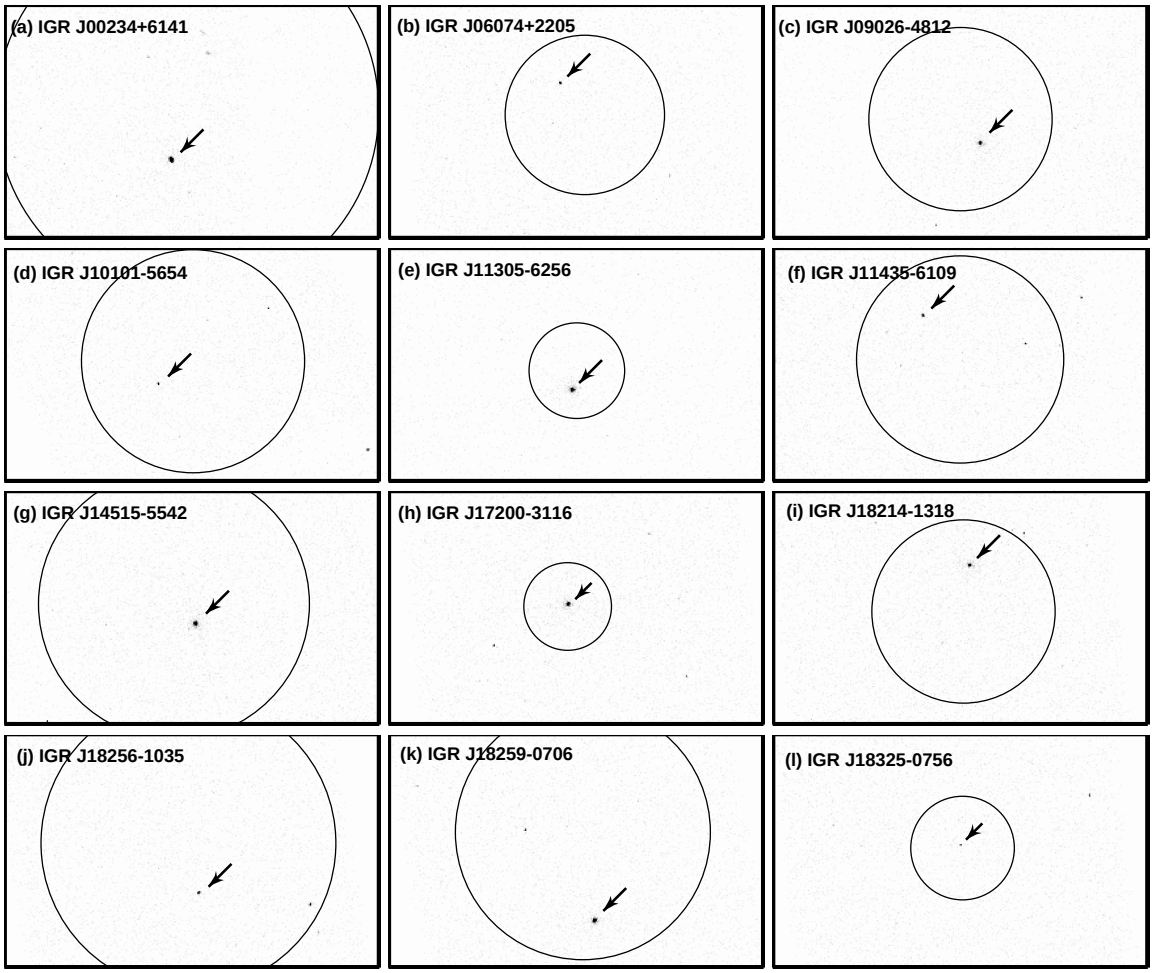

FIG. 1.— *Chandra* 0.3–10 keV images of the 12 IGR-source fields taken with the ACIS instrument. The 90% confidence *INTEGRAL* error circles are shown in each case, and their radii are (a) 4′.8, (b) 2′, (c) 2′, (d) 2′.8, (e) 1′.2, (f) 2′.6, (g) 3′.4, (h) 1′, (i) 2′.3, (j) 3′.7, (k) 3′.2, and (l) 1′.3. The images have been re-binned by a factor of 4, giving 2″ pixels. The images are oriented so that North is up and East is to the left. Arrows point to the brightest *Chandra* source detected in each observation, and these are very likely the soft X-ray counterparts to the IGR sources. For the brightest and faintest sources, respectively, 2,200 and 30 counts were detected by *Chandra*.

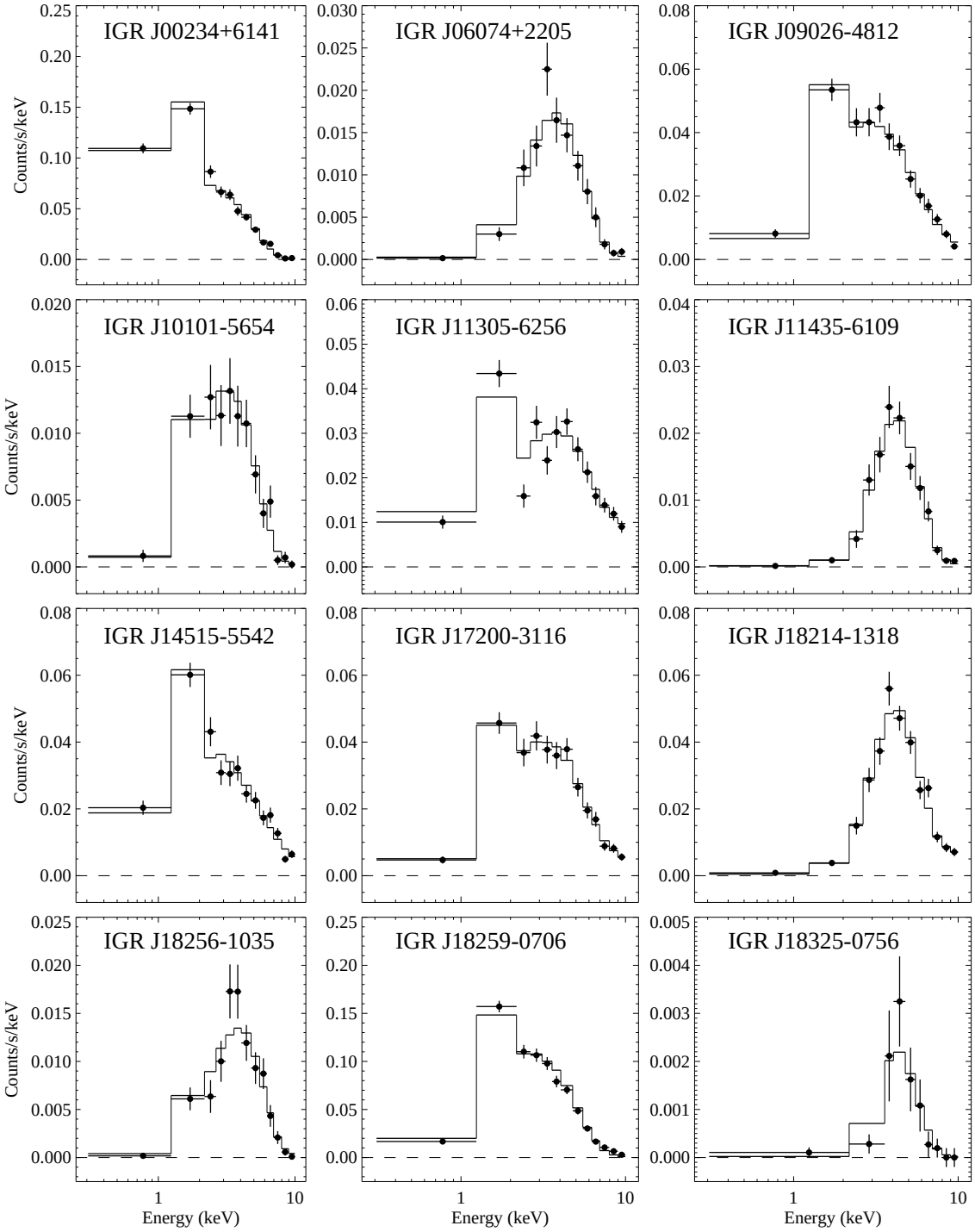

FIG. 2.— *Chandra* 0.3–10 keV spectra of the 12 IGR sources taken with the ACIS instrument. The spectra are fitted with an absorbed power-law model, and photon pile-up must be included in the modeling for 5 of the sources. The model (and pile-up) parameters are given in Table 4.

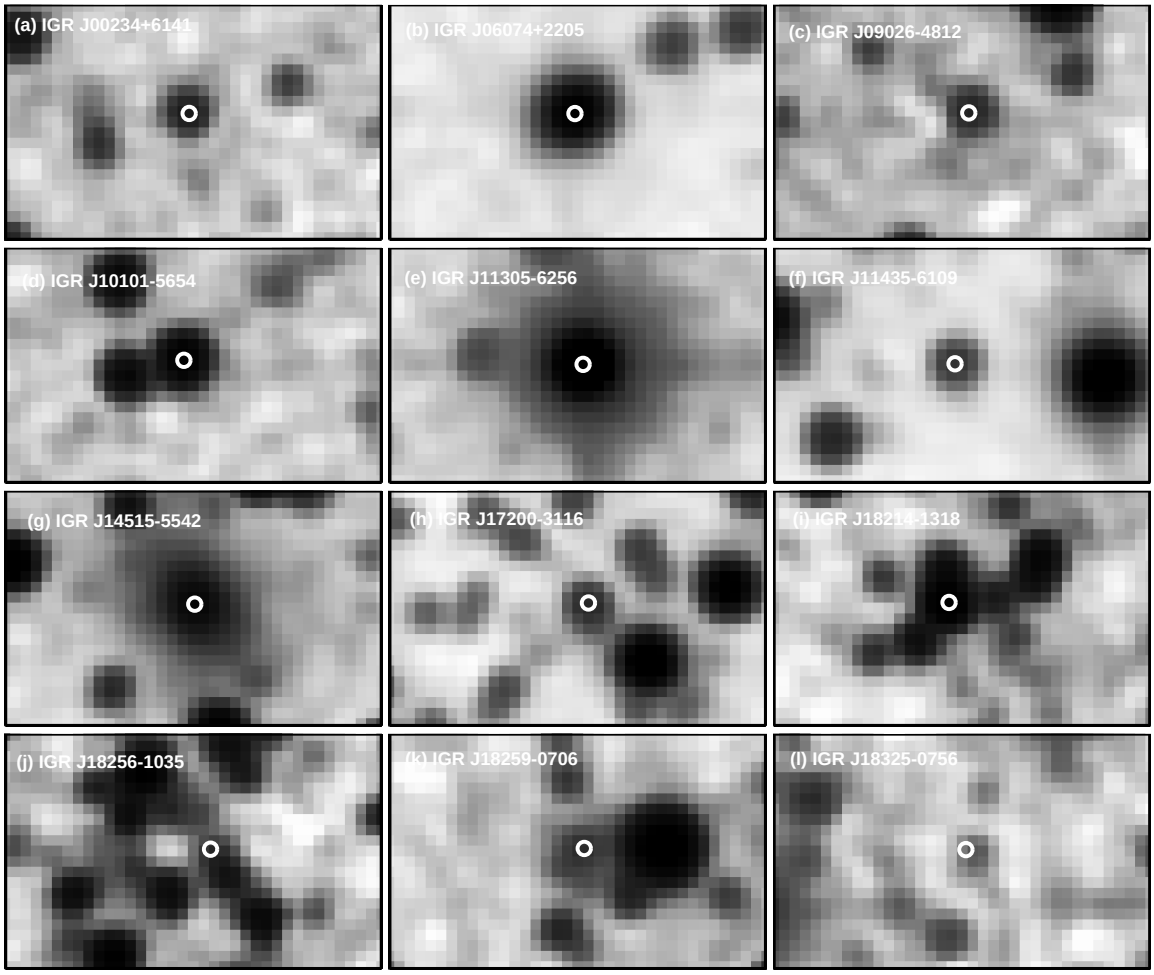

FIG. 3.— 2MASS *J*-band images of the 12 IGR-source fields. The white circle marks the 90% confidence 0″.64 *Chandra* error circle. The images are oriented so that North is up and East is to the left. The pixel sizes for the 2MASS images are 1″, and the size of each image is 34″ in the East-West direction and 22″ in the North-South direction.

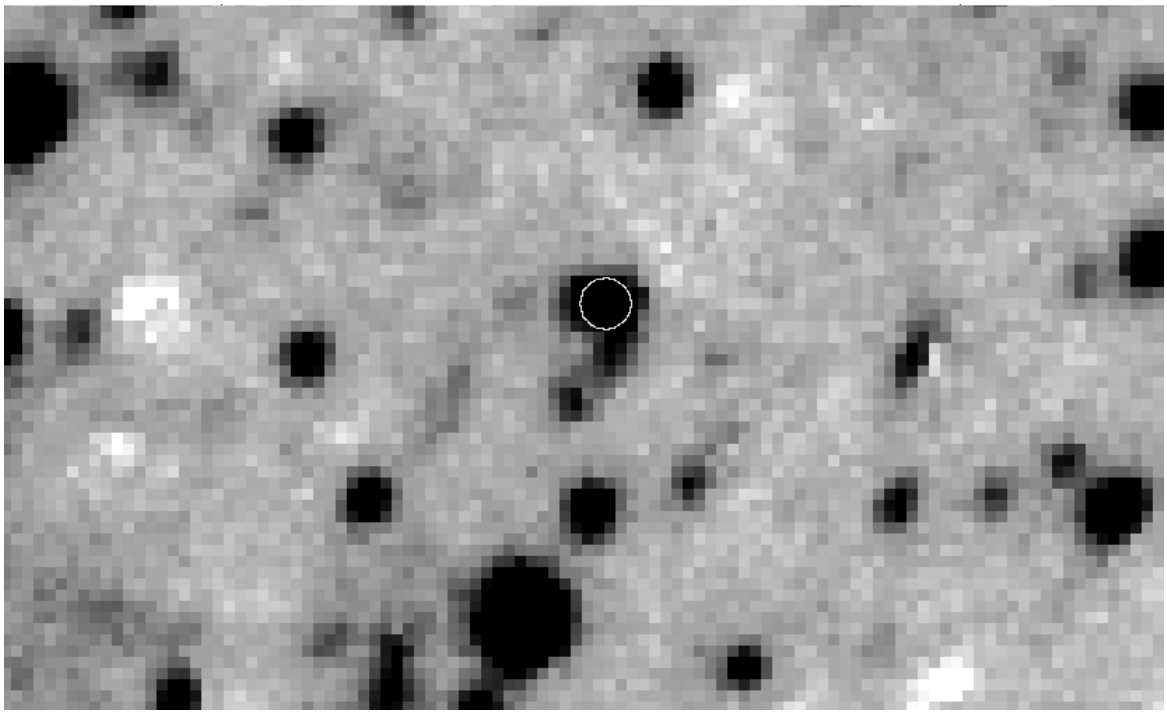

FIG. 4.— K_s-band image of the IGR J18325–0756 field taken with the SofI instrument on the 3.5 meter New Technology Telescope (NTT). The image is oriented so that North is up and East is to the left. The pixel size is $0''.288$. The white circle marks the position of the *Chandra* source CXOU J183228.3–075641, and its position is consistent with that of 2MASS J18322828–0756420, which has a K_s-magnitude of 14.27 ± 0.08.